Journal of Applied Polymer Science

Hybrid organosiloxane coatings containing epoxide precursors for protecting mild steel against corrosion in a saline medium

Rami Suleiman,[1] Mohammed Estaitie,[2] Mohammad Mizanurahman[1]

[1]Center of Research Excellence in Corrosion, King Fahd University of Petroleum & Minerals (KFUPM), Dhahran, 31261, Saudi Arabia

[2]Chemistry Department, King Fahd University of Petroleum & Minerals (KFUPM), Dhahran, 31261, Saudi Arabia

Correspondence to: R. Suleiman (E-mail: ramismob@kfupm.edu.sa)

ABSTRACT: Hybrid organic–inorganic materials made from sol–gel precursors can be used as anticorrosion barriers on metal substrates. The modification of epoxy resins with silicones is an interesting approach toward the synthesis of hybrid materials that combine the advantages offered by epoxy resins with those of silicones. In this study, novel hybrid epoxy-silicon materials were synthesized using sol–gel chemistry and subsequently functionalized with 4,4′-methylenebis(phenyl isocyanate), incorporating urethane functionality into the final polymer. The study screened five different epoxide precursors for use in the synthesis of the new hybrid materials and optimizing their anticorrosion properties. Spectral characterization confirms the proposed chemical structures of the newly synthesized polymers. The newly developed polymers were painted on mild steel panels, thermally cured, and their thermal, surface morphological, adhesion, and anticorrosion properties were fully characterized. The new coatings were found to have excellent thermal stability and adherence properties to steel surface. The results of corrosion testing on coated steel panels following long-term immersion in a 3.5 wt % aqueous NaCl medium revealed that the polymer prepared using the epoxide precursor bisphenol A diglycidyl ether provided the best anticorrosion protection property among the synthesized polymers. This could be attributed to the excellent integrity and crosslink density properties in addition to the lack of microdefects in the surface of this coated sample as confirmed by scanning electron microscopy analyses. The newly prepared hybrid coatings reported in this study are very promising as an alternative to toxic chromate-based coatings. © 2016 Wiley Periodicals, Inc. J. Appl. Polym. Sci. **2016**, *133*, 43947.

KEYWORDS: applications; coatings; properties and characterization

Received 30 January 2016; accepted 22 May 2016

DOI: 10.1002/app.43947

INTRODUCTION

There is currently considerable research directed toward the development of novel high-performance polymers. When applied to metal surfaces, specific polymers have excellent mechanical, thermal, and anticorrosive characteristics that are ideal for applications as coatings in adverse environmental conditions, especially the saltwater environment.[1–3] This environment is considered one of the most corrosive natural environments, as it contains the highly corrosive chloride ion. Research in inorganic–organic hybrid resins has led to creative polymers with unique features for specific applications.[4–6] These polymeric materials are potential alternatives to the existing highly toxic chromate-based coatings. The organic component of a hybrid sol–gel coating imparts a low curing temperature while retaining flexibility and high density; the inorganic components, usually added as metal alkoxides, enhance the coating's mechanical properties, such as hardness and substrate adhesion.[7–10] Epoxy-modified polysiloxane coatings are type of organic–inorganic hybrid resins that are having promising anticorrosion properties.[11,12] These materials are normally prepared by the combination of epoxy precursors/resins, polysiloxanes, organosiloxanes, and difunctional aminosilane hardeners, and provide increased protection from weathering and ultraviolet light, in addition to improved chemical resistance and anticorrosion properties.[13–15] The corrosion resistance of epoxy-modified polysiloxane coatings has been attributed to their physical barrier properties, which restrict the penetration of electrolytes toward the metallic substrate.[16] The chemical structure and organic functionality of silanes can be varied and optimized to achieve the maximum effect in terms of the hydrolytic stability of the interface, desired hydrophobicity or adhesion properties.[17]

Additional Supporting Information may be found in the online version of this article.

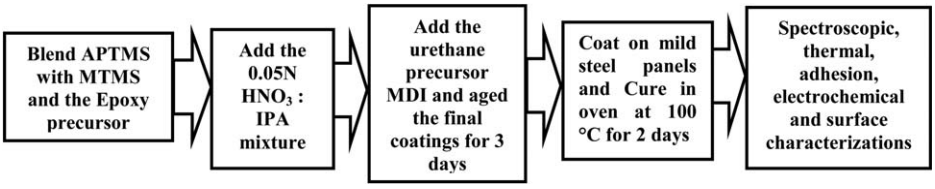

Scheme 1. Summarized process scheme for the development of the new coatings in this study.

Our group has previously reported the synthesis of epoxy-siliconized coatings with urethane functionalities.[13] In that work, we reported the effect of varying the type of amino-functionalized crosslinker on the anticorrosion properties of epoxy-siliconized coatings with urethane functionalities in a saline medium. The crosslinker (3-aminopropyl)trimethoxysilane (APTMS) was found to produce the best anticorrosive coating.[13] In order to further expand on this previous work and due to the major effect of the type of epoxide precursor on the properties of the hybrid sol–gel system, here we report the use of different epoxide precursors for the synthesis of novel hybrid materials as anticorrosive coatings for metal surfaces. To achieve this, the crosslinker APTMS was covalently coupled to five epoxy compounds of different organic functionalities: poly(propylene glycol) diglycidyl ether (Epox1), butyl glycidyl ether (Epox2), bisphenol A diglycidyl ether (Epox3), 1,2,7,8-diepoxyoctane (Epox4), and (3-glycidyloxypropyl)trimethoxysilane (Epox5). Methyltrimethoxysilane (MTMS) silane precursor was also reacted with above reaction mixture in order to induce more hydrophobicity to the desired coating while retaining high crosslink density. Urethane functionalities were induced in the resulting cross-linked epoxy-silicon products by adding the 4,4′-methylenebis(phenyl isocyanate) (MDI) urethane precursor. We aimed by imparting the hybrid epoxy-siliconized materials with urethane functionalities to enhance different desired properties in our final coatings such as the adhesion, chemical resistance, and hydrolytic stability.[18] The chemical structures for the aforementioned molecules are shown in the Supporting Information. The chemical structures of the prepared organosiloxane hybrid polymers were investigated using Fourier transform infrared spectroscopy (FTIR) and nuclear magnetic resonance (NMR). The polymers were coated onto mild steel (the reason behind selecting mild steel for this study is the extensive use of this metal substrate in various industrial fields such as marine applications, nuclear power and fossil fuel power plants, transportation, chemical processing, petroleum production and refining, pipelines, mining, construction, and metal-processing equipment) panels and thermally cured. The thermal properties of the coated films were characterized via thermogravimetric analysis (TGA), and their surface morphological properties were studied using water contact angles and scanning electron microscopy (SEM) techniques. Finally, the corrosion protection properties for the new coatings in 3.5 wt % NaCl medium were evaluated using electrochemical impedance spectroscopy (EIS) and polarization studies. The whole development process of the newly developed coatings in this study is summarized in Scheme 1.

EXPERIMENTAL

Materials

All chemicals [MTMS, APTMS, poly(propylene glycol) diglycidyl ether (DER732), butyl glycidyl ether, bisphenol A diglycidyl ether, 1,2,7,8-Diepoxyoctane, (3-Glycidyloxypropyl) trimethoxysilane (GPTMS),MDI, and isopropyl alcohol] used to synthesize the hybrid epoxy-silicon coatings were purchased from Sigma-Aldrich (USA). Nitric acid (HNO_3) and sodium chloride (NaCl) was purchased from Loba Chemie, India. Distilled water was used in preparing the diluted acid and sodium chloride solutions.

Synthesis of Hybrid Materials

The hybrid materials were prepared by mixing 5 mL of APTMS crosslinker with 10 mL of MTMS for 30 min, and the mixture was then mixed with 2 mL of the selected epoxide (Epox1 to Epox5) for 1 h under stirring in room temperature and open to air. To this solution was added 1 mL of 0.05 *N* HNO_3:isopropanol dropwise and the resultant mixture was stirred overnight. Finally, 0.5 g of MDI was added to the reaction mixture, and the final product was aged for 72 h under room temperature. These produced materials were hereafter termed C1–C5, which contain Epox1–Epox5, respectively. It is worth mentioning here that the work concerning changes in crosslink density via changing the ratios of the reacting materials and reaction conditions in is in progress and will be published at a later date.

Coating Procedure

The S-36 mild steel Q-panels (Q-Lab Company, US) of 76 × 152 × 0.8 mm dimension (used as received) were cleaned ultrasonically for 10 min using absolute ethanol and air-dried before being coated with the hybrid polymers. The hybrid coatings were prepared using a K101 control coater (UK). The thickness of all produced films (around 50 μm) was controlled using the blue metal bar. The coated samples were dried for an hour in open air and at room temperature and then cured at 100 °C for 48 h in an oven and air atmosphere as optimized curing conditions. Unfortunately, materials C4 and C5 formed complete gels after one week of aging (Unlike materials C1–C3 which showed a continuous liquid phase stability) so these two materials were not investigated further in this study.

Characterization

A Nicolet 6700 Fourier transform infrared spectrometer (Thermo Electron Corporation, UK) equipped with a DTGS KBr detector was utilized to characterize the chemical structure of the prepared hybrid polymers and their precursors. The spectra for all of these materials were collected in transmittance mode within the 4000–400 cm^{-1} range over 64 scans and using the attenuated total reflectance sampling tool. Proton and carbon-13 NMR spectra for the prepared liquid hybrid polymers and their precursors were recorded on a 500 MHz Joel 1500 NMR instrument. Deuterated dimethyl sulfoxide (DMSO-d_6) containing 0.1% (v/v) tetramethylsilane (TMS) was used to solvate the fresh liquid sol–gel polymeric samples, and chemical

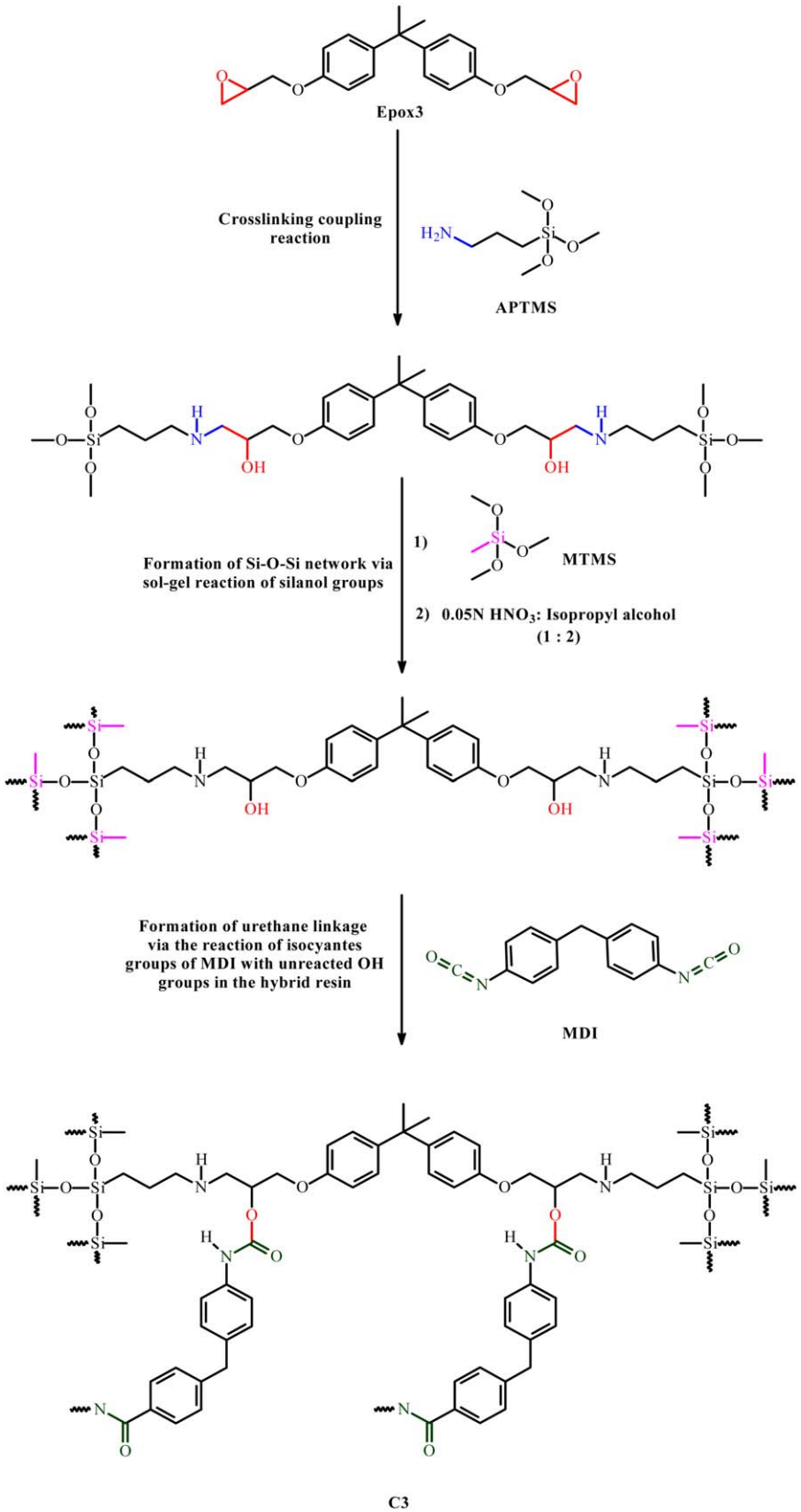

Figure 1. Generic reactions involved in the synthesis of coating C3. [Color figure can be viewed in the online issue, which is available at wileyonlinelibrary.com.]

shifts (δ) were reported in ppm relative to TMS. The thermogravimetric data were obtained from a thermogravimetry analyzer (Perkin-Elmer TGA 7, US) performed under a dry nitrogen atmosphere over a temperature range of 25–700 °C using a heating rate of 10 °C min^{-1}.

Electrochemical data were collected using a potentiostatic–galvanostatic GAMRY3000 corrosion measurement system (GAMRY, USA). The electrochemical cell used for the Tafel polarization study consisted of the a mild steel hybrid-coated panel as the working electrode, a graphite rod as the counter electrode, a standard calomel electrode (SCE) as the reference electrode, and 3.5 wt % aqueous sodium chloride solution as the electrolyte. Electrochemical surface masks (GAMRY, USA) with an area of 10 cm^2 were used to define a specific area for analysis. For Tafel polarization measurements the potential was scanned from −0.25 V to 0.25 V with respect to the open circuit potential at a potential sweep rate of 1 mV s^{-1}. The protective behavior against corrosion was also studied by conducting electrochemical impedance analysis, and data were collected using a GAMRY3000 potentiostat with a frequency range between 100 kHz and 10 mHz. The number of points taken was 10/decade with an AC voltage of 10 mV. Data fitting and electrochemical simulations were carried out using the EChem Analyst software.

In order to determine the effect of prolonged immersion in sodium chloride solution on the hybrid polymer coated samples, the subsequent surface and cross-section morphology was studied using a JEOL JSM-6610 LV SEM. Water contact angles (θ_w) of coated samples before and after immersion in salt medium were measured using the pendant drop method and a DSA30 instrument (KRÜSS, Germany), and mean value of three measurement was plotted. The adhesion strengths of all prepared coatings on mild steel panels were determined using a hydraulic adhesion tester (Paint Test Equipment, UK).The tested area of the coated panels was 3 cm^2.

RESULTS AND DISCUSSION

The preparation of the hybrid polymers involves a crosslinking coupling reaction between the epoxy groups in the epoxide precursor and the amino group in APTMS, followed by hydrolysis and polycondensation reactions of the silanol groups in APTMS and MTMS to form the inorganic polymeric segment. Finally, the reaction of the isocyanate groups in MDI with unreacted —OH groups in the hybrid polymer will produce urethane linkages in the final polymer. Generic reactions involved in the synthesis of the hybrid polymer C3 (as an example) are summarized in Figure 1. The use of APTMS coupling agent as a crosslinker in the synthesis of the new hybrid polymers is expected to increase the crosslink density and thus obtain stronger interfacial interactions between the inorganic and organic components. The network formation in these hybrid coatings is mainly controlled by the relative rates of formation of the organic and inorganic components and the synergy between them.[13] Therefore, understanding the nature of chemical reactions occurred during the sol–gel processing and network growth is highly required for optimizing the synergy between the two components and ultimately the coating properties. High crosslink density is always targeted for any newly developed protective coating in order for this property to aid in prohibiting the passage of corrosive ions through coating to the surface of metals. It will also enhance its mechanical properties, thermal stability, resistance to oxidation, and stable properties. The desired crosslink density can be achieved through the careful selection of the network formation precursors and the insurance of their complete reaction. Thermal curing is also a significant adopted technique for enhancing the crosslink density of most of the newly prepared coatings. The motivation behind testing five different epoxide precursors in our study is to screen the effect different organic moieties on the barrier properties of the final hybrid polymeric product. An insight into the proposed chemical structure of the final hybrid polymers has been achieved using FTIR and NMR spectroscopic techniques.

Structural Characterization of the Bulk Hybrid Polymers

Qualitative information on the occurrence of crosslinking and polycondensation reactions during the preparation of the hybrid polymers C1–C3 can be obtained by comparing their IR spectrum to the IR spectra of the used precursors (Table I and Supporting Information). Taking C3 as an example, the strong peak at 1091 cm^{-1} in its IR spectrum is attributed to the formation of Si—O—Si bonds, which confirms the hydrolysis and polycondensation of the silanol groups. The disappearance of the absorbance peak in the IR spectrum of Epox3 at 913 cm^{-1} (epoxy bending) confirms epoxy conversion and covalent attachment of Epox3 to the silane group.[19] The absorption peaks at 1548 and 1679 cm^{-1} correspond to the C—N and C═O groups of the urethane moiety, respectively. Further evidence for the formation of the urethane group is indicated by the absence of a peak at 2292 cm^{-1}, which would correspond to unreacted isocyanate groups in MDI.[20] The broad peak at 3355 cm^{-1} is attributed either to the NH_2 group or to unreacted silanol —OH groups. The peak at 1602 cm^{-1} corresponds to the C═C bond in the phenyl rings of the polymer.[21] The strong peak at 2971 cm^{-1} is assigned to the C—H bond of phenyl rings. The FTIR spectra of coatings C1 and C2 (Supporting Information) show the presence of the characteristic peaks described above with minor frequency shifts due to the effect of the epoxy precursor.

The chemical structures of the newly prepared hybrid polymers were further verified using the results of ^{1}H-NMR and ^{13}C-NMR analysis (Table I and Supporting Information). The above chemical transformations proved with the FTIR techniques can also be followed using the NMR techniques. The disappearance of the oxirane proton peaks at 2.67 and 2.81 ppm in the ^{1}H-NMR spectrum of C3 (as an example) reveals clearly the coupling reaction between the epoxide groups in Epox3 and the amine group in APTMS. This is also confirmed by observing that the chemical shift of the proton in the N—CH_2 group in the APTMS monomer (2.02 ppm) has now shifted downfield in C3 (2.51 ppm). The presence of a small signal at 3.03 ppm in C3 indicates that not all of the —OCH_3 groups in APTMS were hydrolyzed during the sol–gel reaction. These residual methoxy groups might be eliminated following thermal curing in air.[17] The aromatic protons in C3 are now no longer symmetrical, and their chemical shifts range from 6.78 to 7.26 ppm confirming the reaction of Epox3.

Table I. The Main IR, ^{1}H-NMR, and ^{13}C-NMR Characteristic Signals of the Prepared Hybrid Polymers and their Precursors

	Characteristic signals		
	IR (cm^{-1})	^{1}H-NMR (δ ppm)	^{13}C-NMR (δ ppm)
APTMS	3377 (νN—H), 1191 (νSi—CH_2)	$CDCl_3$t 2.01 (CH_2—N), s 2.90 (OCH_3)	5.8 (Si—CH_2), 44.5 (CH_2—N), 49.9 (OCH_3)
MTMS	2971 (νC—H), 1275 (νSi—CH_3)	$CDCl_3$s 0.19 (Si—CH_3), s 3.58	−8.9 (Si—CH_3), 50.1 (OCH_3)
Epox1	2973 (νC—H), 906 (νOxirane)	$CDCl_3$d 1.15 (CH_3CH), 3.91 (CH—O)	18.5 (CH_3CH), 43.8 (CH_2O, Oxirane), 50.3 (CHO, Oxirane)
Epox2	910 (νOxirane)	$CDCl_3$m 1.38 (CH_3CH_2), t 2.79 (CHO, Oxirane)	44.2 (CH_2O, Oxirane), 71.4 (OCH_2CH)
Epox3	2967 (νC—H arom.), 1608 (νC=C arom.)	DMSO-*d6*s 1.58 (CH_3C)	43.8 (CH_2O, Oxirane), 156.0 (C—O, arom.)
MDI	2292 (νNCO), 1606 (νC=C arom.)	DMSO-*d6*dd 7.06 (CH, arom.) dd 7.31 (CH, arom.)	124.2 (NCO), 152.5 (C—N, arom.)
C1	3359 (νN—H), 2972 (νC—H arom.), 1663 (νC=O, Urethane), 1600 ((νC—N), 1093 (νSi—O—Si)	DMSO-*d6*s 0.58 (Si—CH_3), s 3.04 (OCH_3), s 7.24 (CH, arom.)	−8.9 (Si—CH_3), 17.2 (CH_3CH), 138.8 (C—N, arom.)
C2	2970 (νC—H arom.), 1713 (νC=O, Urethane), 1091 (νSi—O—Si)	DMSO-*d6*bs 0.46 (Si—CH_3), m 4.29 (OCH_2CH)	−8.8 (Si—CH_3), 155.3 and 156.0 (CO, Urethane)
C3	3355 (νN—H), 1679 (νC=O, Urethane), 1091 (νSi—O—Si)	DMSO-*d6*t 2.51 (NCH_2CH_2), s 7.26 (CH, arom.)	70.8 (HCO), 155.4 and 156.6 (CO, Urethane)

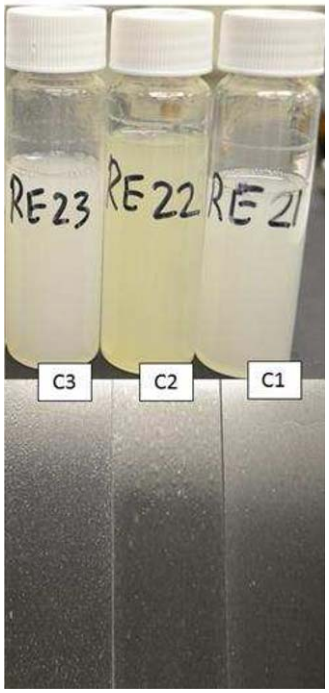

Figure 2. Physical appearance of all hybrid polymer samples after aging for 72 h (top) and the coated samples after thermal curing at 100 °C for 48 h (bottom). [Color figure can be viewed in the online issue, which is available at wileyonlinelibrary.com.]

The corresponding ^{13}C-NMR spectrum of C3 shows that the carbon in —$SiCH_2$ has shifted upfield from 5.8 ppm in the APTMS monomer to −7.8 ppm in C3. This confirms the coupling reaction of the amine group to the oxirane ring. The opening of the oxirane ring can be proven also by the appearance of the two peaks at 68.3 and 70.8 ppm which correspond to the two carbon atoms of the oxirane ring after opening. The peaks at 155.4–156.6 ppm correspond to different urethane carbonyls in C3 confirming the reaction of the isocyanate groups in MDI (no peaks corresponding to the isocyanate carbons are observed in the range of 124.2–129.4 ppm).

Overall, spectroscopic characterization provided strong evidence of the successful preparation of hybrid polymers that contained all starting materials, covalently linked together by the expected bonds. However, the chemical structure of a sol–gel material does not necessarily guarantee that the given material can be used to produce high-quality coatings. Therefore, careful characterization of the cured coatings was also important. The surfaces of all coated samples after curing appear homogenous and intact with no sign of immediate corrosion (Figure 2), except for sample C2, which showed some inhomogeneity in the surface of its coated sample. The digital photographs of the cured samples reveal also a potential scalability of our newly prepared coatings on large metal surfaces.

Adhesion Characterization

The adhesion of the coating depends on the nature of the substrate, as well as on the coating formulation. It is expected for our newly synthesized to adhere to steel surface through a chemical bonding between the unreacted silanol groups and

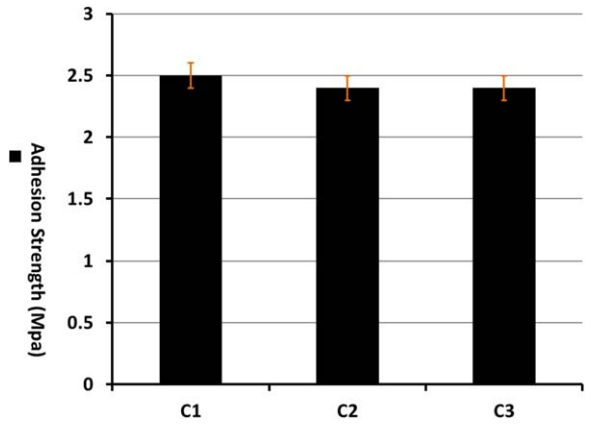

Figure 3. Adhesion strength (in MPa) of the hybrid coatings. [Color figure can be viewed in the online issue, which is available at wileyonlinelibrary.com.]

hydroxyl groups of the steel.[22,23] Figure 3 shows the results of the adhesion test of coatings C1–C3. These results indicate that all coatings have excellent adherence to the steel substrate comparing to other hybrid sol–gel coatings reported in literature.[13] The enhancement of the integrity property of hybrid sol–gel coatings would highly promote their adherence property to metal surfaces.[24]

Thermal Characterization

TGA is an important technique for studying the thermal and/or oxidative stabilities of hybrid polymeric materials. TGA measurements provide valuable information that can be used to select hybrid materials for certain end-use applications, to predict their performance and improve their quality.[25] TGA was used to measure the changes in the weight of the hybrid coatings C1–C3 as a function of temperature in a controlled nitrogen atmosphere. TGA curves for the hybrid sol–gel materials are shown in Figure 4. The first region in the curve, from room temperature to approximately 200 °C, is due to the evaporation of alcohol and water. The TGA curves show strong weight losses between 200 and 300 °C, which can be attributed to the release of organic matter and residual monomers. The next weight loss between 300 and 550 °C is ascribed to pyrolysis of organic chains and adjoining end groups and units, and the final minor weight loss at 550–700 °C may be attributed to the partial decomposition of silica-bonded or entrapped polymeric segments.[13] The curves reveal that coating C3 might has higher molecular weight, crosslinking density and thermal stability compared to C1 and C2.[11]

Next, the corrosion protection performances of the hybrid coated samples in saline medium were evaluated. This has been achieved by immersing the steel-coated panels continuously in 3.5 wt % NaCl solution and conducting the required morphological and electrochemical tests at certain times of immersion. This electrolytic solution is used extensively in corrosion testing as its chloride content is very close to the seawater content. Figure 5 shows digital photographs of the hybrid-coated samples before and after 144 h of continuous immersion in 3.5 wt % NaCl. The presence of general corrosion phenomena can be seen on significant areas of the surface for samples C1 and C2. Conversely, the surface of sample C3 remains unaffected by immersion with the exception of small areas of exfoliation and salt particles adsorbed on the surface.

Surface Properties and Morphology

The hydrophobicity of the coated samples is considered as one of the contributing parameters to the barrier properties of the coating and ultimately its anticorrosion performance.[17,26] The degree of hydrophobicity of surfaces can be determined using aqueous contact angle testing. Data in Figure 6 reveal that the surfaces of all coated samples prepared in this study are hydrophilic (they have a contact angle of less than 90°) before immersion in the chloride solution. The use of epoxy precursors and their subsequent ring opening reaction is expected to contribute to the hydrophilic character of the final prepared hybrid polymers. In principle, the drop in the contact angle values of coated steel samples after prolong immersion in salt medium is a correlated sign to the wetting of their surfaces and the onset of corrosion process. Although the surface of sample C3 shows the least hydrophobic character (a contact angle of 55°) among all samples before immersion, it exhibits the lowest drop in hydrophobicity after immersion, which explains the excellent barrier properties of this coating shown in Figure 5.

Figure 7 shows the SEM images of the top surface of all hybrid coatings after immersing them continuously in 3.5 wt % NaCl for 144 h. No cracks or micro-defects can be observed in the whole surface of C3 sample which might explain the excellent anticorrosion properties of this coating and support results reported above for this coating. The surface of C1 sample found to be severely covered with salt particles while surface inhomogeneity and defects can be seen on the surface of C2 sample. The SEM cross-sectional images of the steel coated samples (Supporting Information) indicate clearly that all coatings are well-bonded (good adherence) to the surface of the steel since no delamination was observed of the coating layer from the steel. Energy-dispersive X-ray spectroscopy (EDS) analysis of the coating layer of all coated samples (Supporting Information) reveals that these coating are composed mainly of Si, C, and O elements which gives more support to the chemical composition

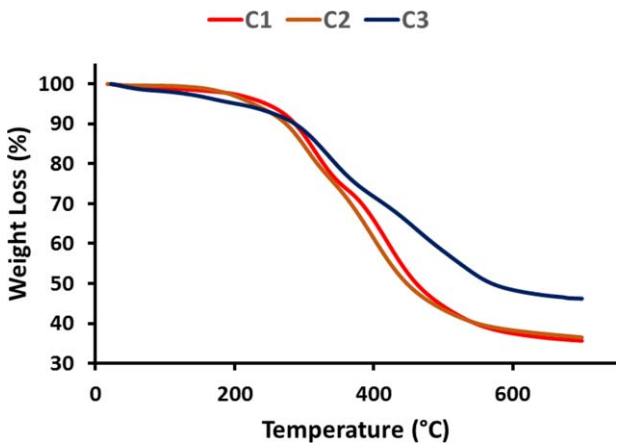

Figure 4. TGA plots of the hybrid coatings. [Color figure can be viewed in the online issue, which is available at wileyonlinelibrary.com.]

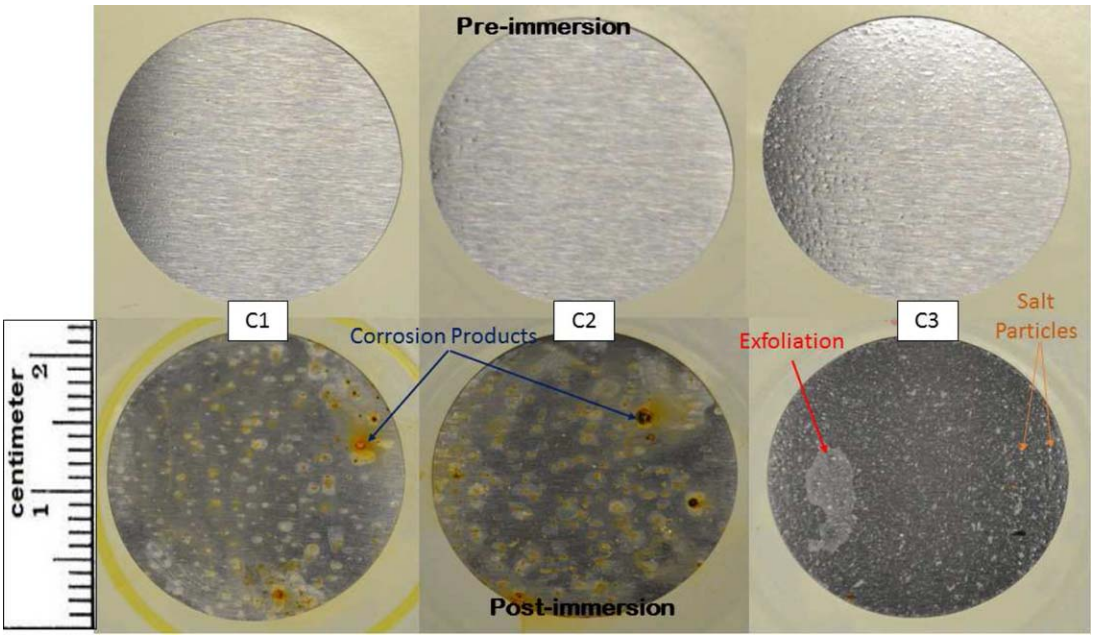

Figure 5. Sections of the panels shown in Figure 5 before and after immersion in 3.5 wt % NaCl for 144 h [The difference in the color of coated surfaces before and after immersion in salt medium is due to the different in lighting conditions while taking the photos]. [Color figure can be viewed in the online issue, which is available at wileyonlinelibrary.com.]

we proposed earlier in this manuscript for our newly prepared hybrid sol–gel materials.

Electrochemical Corrosion Test of the Hybrid Coatings

EIS is a widely used technique to characterize the behavior of coated metals immersed in aqueous electrolyte environments.[27–29] EIS is ideally suited to detecting surface changes after relatively short exposure times compared to traditional mechanical or visual methods.[27] EIS was carried out to evaluate the corrosion protection properties of hybrid-coated samples in 3.5 wt % aqueous NaCl solution. Figure 8(a) shows the Nyquist plots of impedance measurements for C1–C3 hybrid coatings taken during 24 days of continuous immersion in the 3.5 wt % NaCl solution. The excellent performance and the efficient barrier protection at the beginning of the test can be clearly seen for the C3 coating, where the plot consists of a small semicircle and an open capacitive loop with an impedance value of 4.4×10^6 ohm·cm^2. Wider diameters of Nyquist semicircles are attributed of improved corrosion resistance by better protective coatings.[30] The capacitive loop tends to lean toward the real axis as the time of immersion increases, which means that the coating resistance decreases and the capacitance increases due to electrolyte permeation. The Nyquist diagram [Figure 8(a)-inset] for sample C1 has a larger semicircle diameter than C2, indicating that C1 has superior anticorrosion behavior.

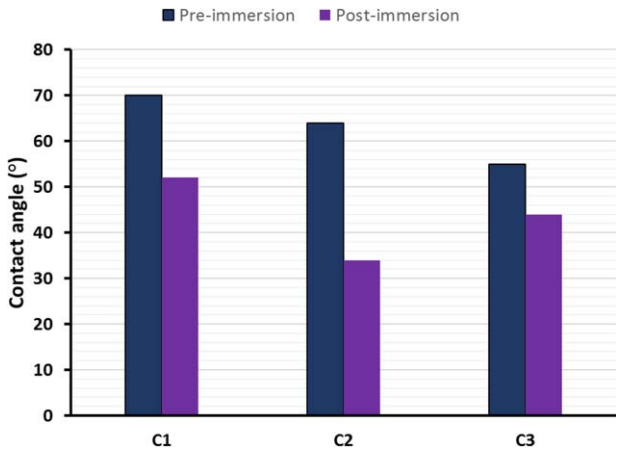

Figure 6. Mean contact angle of each coated sample pre- and post-immersion in 3.5 wt % NaCl for 144 h. [Color figure can be viewed in the online issue, which is available at wileyonlinelibrary.com.]

When the exposure time in the saline solution is increased to 144 h, the performance of the hybrid epoxy-siliconized coatings continued to follow the rank: C3 > C1 > C2. Three semicircles, indicating three time constants, are shown for the C3 coating [Figure 8(b)]. Although the impedance value of this coating is not relatively high (3.5×10^5 ohm cm^2) at this relatively long immersion time, it is still predicted a promising performance for C3 in real marine environment. For samples C1 and C2, there is the presence of a large semicircle at low frequencies in the Nyquist plot [Figure 8(b)-inset], suggesting the onset of electrochemical reactions at the metal/coating interface.[31] This might be attributed to the presence of micropores or cracks in the surface of these coated samples. The relatively high resistance of the C3 coating and its stability over a long immersion period suggests a high crosslink density for this coating and confirm its barrier protection properties which correlates with the conclusions drawn from the TGA analyses. The low barrier properties of C2 may be attributed to the weak crosslink density of this hybrid materials which arise from the use of epoxide precursor of one epoxy group in preparing it comparing to the two other hybrid materials C1

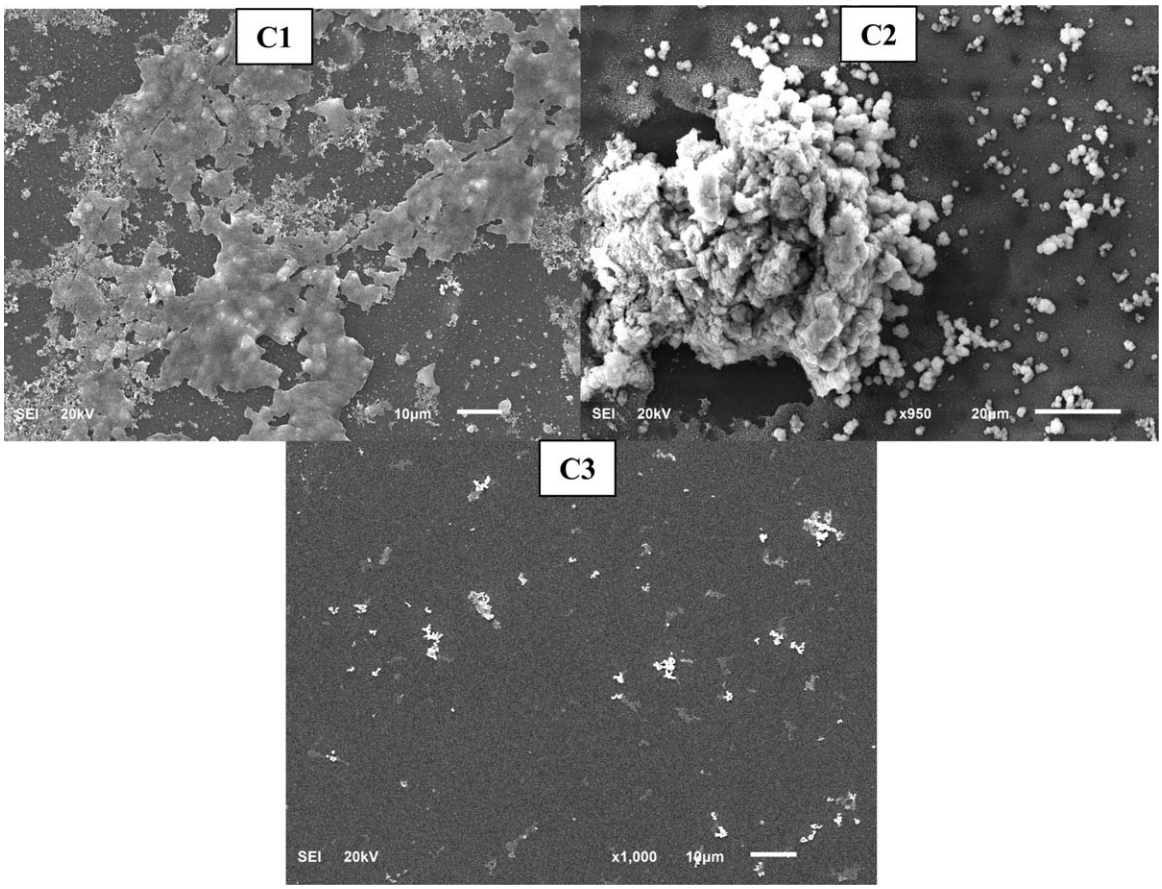

Figure 7. SEM micrograph of the top surface of the hybrid-coated samples immersed in 3.5 wt % NaCl for 144 h.

and C3 which their epoxide precursors have two epoxy groups in their chemical structure.

Figure 9 shows the equivalent circuits for numerical fitting of the EIS data, in order to estimate the evolution of anticorrosion properties for the different coatings. The equivalent circuits are chosen based on the number of time-constants and the goodness of fit. The first equivalent circuit is denoted R(Q(R(QR(QR)))) and consists of three time constants in a parallel configuration. The second equivalent circuit is denoted R(Q(R(QR)))(QR) and consists of two time constants in a

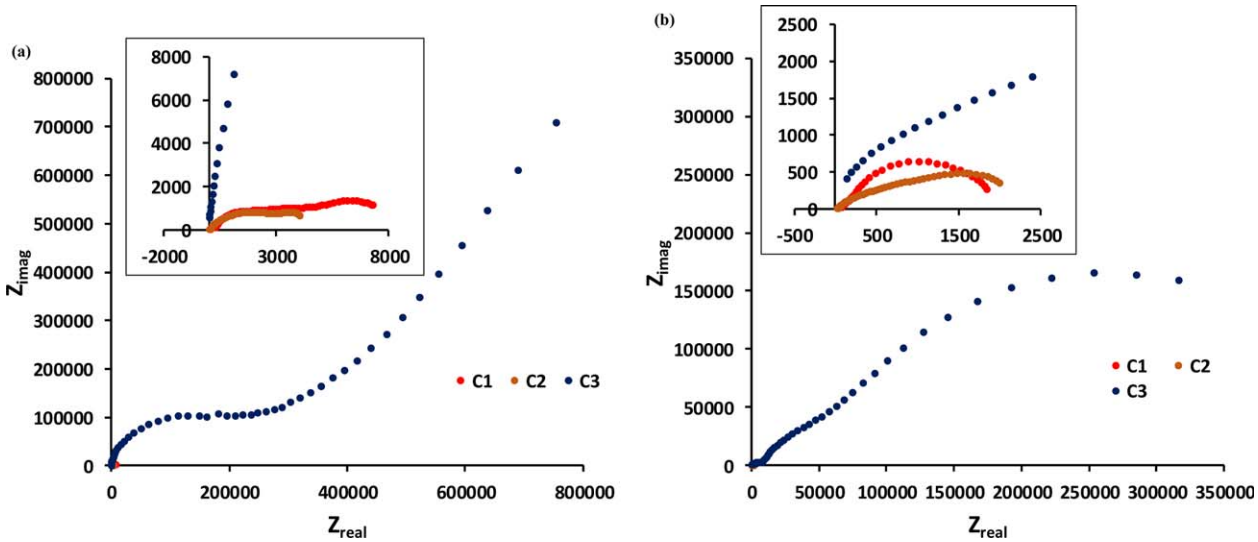

Figure 8. Nyquist plots of the hybrid-coated mild steel samples after, (a) 24 and, (b) 144 h immersion in 3.5 wt % NaCl solution; inset: Nyquist curves showing Z values at higher frequencies. [Color figure can be viewed in the online issue, which is available at wileyonlinelibrary.com.]

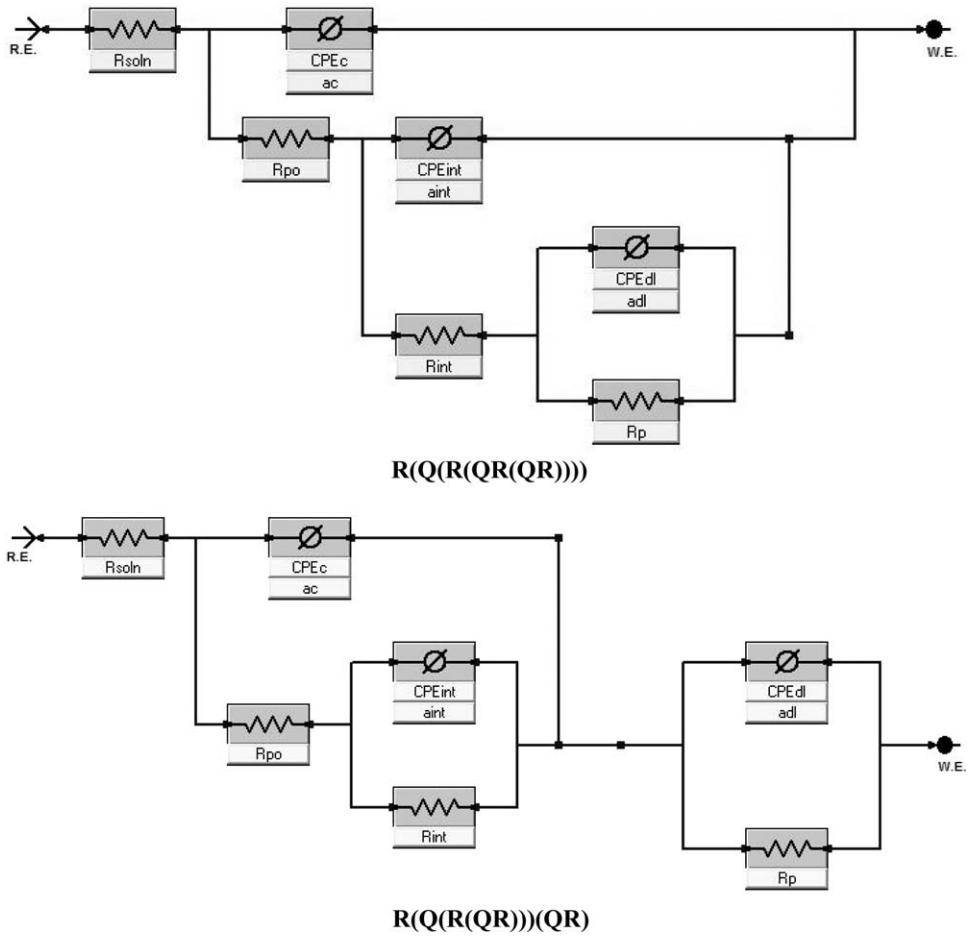

Figure 9. Equivalent circuits used for fitting the EIS data for the hybrid-coated samples.

parallel arrangement followed by a time constant in series. The time constant appears at high frequencies is correlated with the barrier properties of the hybrid coatings, while the time constant correlated the corrosion process appears at lower frequencies and provides ideas on corrosion rates. Constant phase elements (CPE) are used to take into account the non-ideal behavior of the system (phase shift differing from 90°), which can be attributed to the inhomogeneity of the surface of the steel electrode.[32] These equivalent circuits are proposed and established assuming that there is an electrolyte resistance

Table II. Fitting Values Obtained after 24- and 144-h Immersion of Hybrid-Coated Samples in 3.5 wt % NaCl Solution

	C1		C2		C3	
Immersion time (h)	24	144	24	144	24	144
R_{soln} (Ω)	3.0	3.0	3.0	3.0	3.0	3.0
R_{po} (kΩ)	0.275	0.0268	0.0326	0.0247	135.6	6.67
CPE_c (μF cm^{-2} $s^{-(1-\alpha c)}$)	16.79	0.02	0.01	3.84	0.08	0.24
a_c	0.916	1.000	0.993	0.560	0.937	0.682
R_{int} (kΩ)	0.0327	0.0473	1.020	0.691	781.0	99.82
CPEint (μF cm^{-2} $s^{-(1-\alpha c)}$)	0.92	3.1	51.9	162.6	1.1	6.9
a_{int}	0.327	0.933	0.600	0.541	0.358	0.630
Rp (kΩ)	14.65	2.17	533.8	2.07	4718.0	356.8
CPEdl (μF cm^{-2} $s^{-(1-\alpha c)}$)	123.6	713.0	404.6	739.6	1.26	26.1
a_d	0.212	0.645	0.110	0.434	0.867	0.914
Circuit	R(Q(R(QR(QR))))				R(Q(R(QR)))(QR)	

Table III. The Polarization Parameters of all Hybrid-Coated Samples after 144 h Immersion in 3.5 wt % NaCl

Sample	E_{corr} (mV)	I_{corr} (A cm^{-2})	Beta A (V/decade)	Beta C (V/decade)	Corrosion rate (mpy)
C1	−558	5.69×10^{-6}	4.89×10^{-2}	9.09×10^{-2}	2.602
C2	−613	7.62×10^{-6}	7.59×10^{-2}	20.28×10^{-2}	3.481
C3	−426	9.77×10^{-8}	44.30×10^{-2}	18.80×10^{-2}	0.0447

(R_{soln}), a sol–gel layer resistance (R_{po}), and a pore or defect resistance within the sol–gel layer that is represented by R_{po} in parallel with CPE_c. The properties of the intermediate layer are described by a resistance R_{int} and this is in parallel with a capacitor CPEint. A passive layer or film layer (represented by CPEdl and *Rp*) is included to represent a buildup of corrosion products close to the substrate surface. The passive layer may have formed after disbondment of the coating from the substrate.

Table II gives the values obtained for the fitting after 24 or 144 h of immersion in the electrolyte. The R_{po} values of C3 sample are the highest compared to the other two coatings. The low values R_{po} of C1 and C2 samples could be attributed to the presence of multiple microdefects caused by the lack of homogeneity in the bulk of these two coatings on prolonged immersion in the saline electrolyte at room temperature. This inhomogeneity allows free pathways for water and corrosive ions to emerge to the surface of the metal substrate.[33,34] Reduced *Rp* values denotes deterioration of the coating integrity, and the trend in CPEdl values can be employed to support this assertion. An increase in capacitance with immersion time is observed for all coated samples, which is related to water uptake process.[35] Although this tendency is similar for all types of samples, it is stronger for the samples C1 and C2 indicating a higher tendency for water uptake property for the two sol–gel coatings.

Polarization experiments were performed in order to investigate the corrosion tendency of the mild steel substrate after 144 h exposure of the three coated surfaces in the test electrolyte. The polarization curve for the C3-coated mild steel shows significant potential shifts to a nobler region compared with that of C1- and C2-coated metals immersed in 3.5 wt % NaCl (Figure S5 in the Supporting Information). The various polarization parameters, such as corrosion potential (E_{corr}) and corrosion current density (I_{corr}), obtained from cathodic and anodic curves by extrapolation of the Tafel lines, are given in Table III. It is observed that the I_{corr} and E_{corr} values of C3 are the lowest among the other two samples confirming the excellent protection properties of this coating. This correlation between the current density and the barrier properties of immersed coated samples is only valid at prolonged immersion times where the electrochemical reactions taking place are sufficiently controlled by activation. The results of polarization experiments are in full agreement with the EIS analysis reported above, in which sample C3 showed superior anticorrosion performance compared to C1 and C2.

CONCLUSIONS

Hybrid epoxy-siliconized coatings with urethane functionalities were successfully prepared, and their anticorrosion properties on mild steel substrates were evaluated in 3.5% aqueous NaCl solution. EIS and polarization studies revealed that the coating prepared using the epoxide bisphenol A diglycidyl ether (C3) showed the best corrosion protection performance compared with coatings prepared with the two other epoxide precursors (Epox1 and Epox2) which produced hybrid coatings with very less crosslink density and this ultimately affect their barrier properties against the passage of corrosive ions to the surface of steel panels. The use of Epox4 and Epox5 resulted in the formation of hybrid materials of fast gelification behavior. The surfaces of all coated samples were found to be relatively hydrophilic due to the influential contribution of the epoxy component to this surface property. The remarkable thermal, adhesion and barrier properties reported in this study for our newly synthesized coatings make them possible alternatives for commercial and highly toxic chromate-based coatings used for protecting steel surfaces against corrosion.

ACKNOWLEDGMENTS

This project was funded by the National Plan for Science, Technology and Innovation (MARIFAH), King Abdulaziz City for Science and Technology, through the Science & Technology Unit at King Fahd University of Petroleum & Minerals (KFUPM), the Kingdom of Saudi Arabia, award number (14-ADV147-04).

REFERENCES

1. Gupta, P.; Bajpai, M. *Adv. Chem. Eng. Sci.* **2011**, *1*, 133.
2. Borovin, E.; Callone, E.; Ceccato, R.; Quaranta, A.; Dire, S. *Mater. Chem. Phys.* **2014**, *147*, 954.
3. Lakshmi, R. V.; Bharathidasan, T.; Bera, P.; Basu, B. J. *Surf. Coat. Technol.* **2012**, *206*, 3888.
4. Bajpai, P.; Bajpai, M. *Pigment Resin Technol.* **2010**, *39*, 96.
5. Lee, T. J.; Kwon, S. H.; Kim, B. K. *Prog. Org. Coat.* **2014**, *77*, 1111.
6. Roy, A.; Singh, S. S.; Datta, M. K.; Lee, B.; Ohodnicki, J.; Kumta, P. N. *Mater. Sci. Eng. B* **2011**, *176*, 1679.
7. Feng, Z.; Liu, Y.; Thompson, G. E.; Skeldon, P. *Surf. Interface Anal.* **2010**, *42*, 306.
8. Voevodin, N. N.; Grebasch, N. T.; Soto, W. S.; Kasten, L. S.; Grant, J. T.; Arnold, F. E.; Donley, M. S. *Prog. Org. Coat.* **2001**, *41*, 287.
9. Figueira, R. B.; Silva, C. J. R.; Pereira, E. V. *J. Coat. Technol. Res.* **2015**, *12*, 1.
10. Zheludkevich, M. L.; Salvadob, I. M.; Ferreira, M. G. S. *J. Mater. Chem.* **2005**, *15*, 5099.

11. Chattopadhyay, D. K.; Webster, D. C. *Prog. Org. Coat.* **2009**, *66*, 73.
12. Vreugdenhil, A. J.; Gelling, V. J.; Woods, M. E.; Schmelz, J. R.; Enderson, B. P. *Thin Solid Films* **2008**, *517*, 538.
13. Suleiman, R.; Dafalla, H.; El Ali, B. *RSC Adv.* **2015**, *5*, 39155.
14. Bajpai, M.; Sharma, A. *Paint India* **1997**, *47*, 53.
15. Brushwell, W. *Paint India* **1981**, *31*, 11.
16. Wang, H.; Akid, R. *Corros. Sci.* **2007**, *49*, 4491.
17. Eduok, U.; Suleiman, R.; Khaled, M.; Akid, R. *Prog. Org. Coat.* **2016**, *93*, 97.
18. Chen, G.-N.; Chen, K.-N. *J. Appl. Polym. Sci.* **1997**, *63*, 1609.
19. Li, W.; Huang, D.; Xing, X. Y.; Xing, J. Y.; Li, X.; Zhang, J. *J. Appl. Polym. Sci.* **2014**, *131*, DOI: 10.1002/app.41010.
20. Ren, Z.-Y.; Wu, H.-P.; Ma, J.-M.; Ma, D.-Z. *Chin. J. Polym. Sci.* **2004**, *22*, 225.
21. Arasa, M.; Ramis, X.; Salla, J. M.; Mantecón, A.; Serra, A. *J. Polym. Sci. Part A: Polym. Chem.* **2007**, *45*, 2129.
22. Chou, T. P.; Chandrasekaran, C.; Cao, G. Z. *J. Sol-Gel Sci. Technol.* **2003**, *26*, 321.
23. Chou, T. P.; Cao, G. Z. *J. Sol-Gel Sci. Technol.* **2003**, *27*, 31.
24. Palanivelu, S.; Dhanapal, D.; Srinivasan, A. K. *Silicon* **2014**, DOI: 10.1007/s12633-014-9202-6.
25. Thermal Analysis. Available at: http://depts.washington.edu/mseuser/Equipment/RefNotes/TGA_Notes.pdf.
26. Eduok, U.; Suleiman, R. K.; Gittens, J.; Khaled, M. M.; Smith, T. J.; Akid, R.; El Ali, B.; Khalil, A. B. *RSC Adv.* **2015**, *5*, 93818.
27. Suleiman, R.; Mizanurrahman, M.; Alfaifi, N.; El Ali, B.; Akid, R. *Eng. Sci. Technol.* **2013**, *48*, 525.
28. Suleiman, R.; Khaled, M.; Wang, H. *Corros. Eng. Sci. Technol.* **2014**, *49*, 189.
29. Suleiman, R. *Anti-Corros. Meth. Mater.* **2014**, *61*, 423.
30. Pebere, N.; Riera, C.; Dabosi, F. *Electrochim. Acta* **1990**, *35*, 555.
31. Kendig, M.; Mansfeld, F.; Tsai, S. *Corros. Sci.* **1983**, *23*, 317.
32. Kannan, A. G.; Choudhury, N. R.; Dutta, N. K. *J. Electroanal. Chem.* **2010**, *641*, 28.
33. Shakeri, A.; Abdizadeh, H.; Golobostanfard, M. R. *Appl. Surf. Sci.* **2014**, *314*, 711.
34. Juan, D. M. J.; Martinez, I. M.; Hernandez, E. M.; CabedoIzquierdo, L.; Suay, J.; Gurruchaga, M.; Goni, I. *Prog. Org. Coat.* **2014**, *77*, 1799.
35. Collazo, A.; Covelo, A.; Nóvoa, X. R.; Pérez, C. *Prog. Org. Coat.* **2012**, *74*, 334.